Journal of Hazardous Materials 431 (2022) 128594

Contents lists available at ScienceDirect

Journal of Hazardous Materials

journal homepage: www.elsevier.com/locate/jhazmat

# Extracellular vesicles as an alternative copper-secretion mechanism in bacteria

Steeve Lima [a,b,c], Jorge Matinha-Cardoso [a,b], Joaquín Giner-Lamia [d,e,f], Narciso Couto [g], Catarina C. Pacheco [a,b], Francisco J. Florencio [d,h], Phillip C. Wright [i], Paula Tamagnini [a,b,j], Paulo Oliveira [a,b,j,*]

[a] i3S – Instituto de Investigação e Inovação em Saúde, Universidade do Porto, Rua Alfredo Allen, 208, 4200-135 Porto, Portugal
[b] IBMC – Instituto de Biologia Molecular e Celular, Universidade do Porto, Rua Alfredo Allen, 208, 4200-135 Porto, Portugal
[c] MCbiology Doctoral Program, ICBAS – Instituto de Ciências Biomédicas Abel Salazar, Universidade do Porto, Rua de Jorge Viterbo Ferreira, 228, 4050-313 Porto, Portugal
[d] Instituto de Bioquímica Vegetal y Fotosíntesis, Universidad de Sevilla-CSIC C, Américo Vespucio, 49, 41092 Sevilla, Spain
[e] Centro de Biotecnología y Genómica de Plantas, Universidad Politécnica de Madrid (UPM), Instituto Nacional de Investigación y Tecnología Agraria y Alimentaria (INIA), Parque Científico y Tecnológico, UPM Campus de Montegancedo, Ctra, M-40, km 38, 28223 Madrid, Spain
[f] Departamento de Biotecnología-Biología Vegetal, Escuela Técnica Superior de Ingeniería Agronómica, Alimentaria y de Biosistemas, Universidad Politécnica de Madrid (UPM), Campus, Av. Puerta de Hierro, n° 2, 4, 28040 Madrid, Spain
[g] Department of Chemical and Biological Engineering, University of Sheffield, Mappin St, Sheffield City Centre, Sheffield S1 4NL, United Kingdom
[h] Departamento de Bioquímica Vegetal y Biología Molecular, Facultad de Biología, Universidad de Sevilla, Avenida Reina Mercedes s/n, 41012 Sevilla, Spain
[i] University of Southampton, Office of the President and Vice Chancellor B37, University Rd, Highfield, Southampton SO17 1BJ, United Kingdom
[j] Departamento de Biologia, Faculdade de Ciências, Universidade do Porto, Rua do Campo Alegre s/n, 4169-007 Porto, Portugal

## HIGHLIGHTS

- Extracellular vesicles (EVs): overlooked metal resistance mechanism in bacteria.
- Vesiculation is a common response mechanism to copper-induced stressful conditions.
- Cyanobacterial EVs are packaged with metal binding proteins.
- Cyanobacterial EVs work as copper-secreting nanocapsules.

## GRAPHICAL ABSTRACT

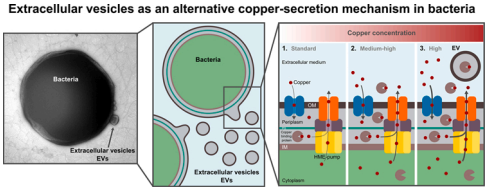


## ARTICLE INFO

*Keywords:*
Metal homeostasis
Copper detoxification mechanisms
Copper secretion
Cyanobacteria
Bacterial extracellular vesicles

## ABSTRACT

Metal homeostasis is fundamental for optimal performance of cell metabolic pathways. Over the course of evolution, several systems emerged to warrant an intracellular metal equilibrium. When exposed to growth-challenging copper concentrations, Gram-negative bacteria quickly activate copper-detoxification mechanisms, dependent on transmembrane-protein complexes and metallochaperones that mediate metal efflux. Here, we show that vesiculation is also a common bacterial response mechanism to high copper concentrations, and that extracellular vesicles (EVs) play a role in transporting copper. We present evidence that bacteria from different ecological niches release copious amounts of EVs when exposed to copper. Along with the activation of the classical detoxification systems, we demonstrate that copper-stressed cells of the cyanobacterium *Synechocystis* sp. PCC6803 release EVs loaded with the copper-binding metallochaperone CopM. Under standard growth conditions, CopM-loaded EVs could also be isolated from a *Synechocystis* strain lacking a functional TolC-protein, which we characterize here as exhibiting a copper-sensitive phenotype. Analyses of *Synechocystis tolC*-mutant's

* Corresponding author at: i3S – Instituto de Investigação e Inovação em Saúde, Universidade do Porto, Rua Alfredo Allen, 208, 4200-135 Porto, Portugal.
*E-mail address:* paulo.oliveira@ibmc.up.pt (P. Oliveira).

https://doi.org/10.1016/j.jhazmat.2022.128594
Received 16 September 2021; Received in revised form 18 February 2022; Accepted 24 February 2022
Available online 26 February 2022
0304-3894/© 2022 Published by Elsevier B.V. This is an open access article under the CC BY license (http://creativecommons.org/licenses/by/4.0/).

EVs isolated from cells cultivated under standard conditions indicated the presence of copper therein, in significantly higher levels as compared to those from the wild-type. Altogether, these results suggest that release of EVs in bacteria represent a novel copper-secretion mechanism, shedding light into alternative mechanisms of bacterial metal resistance.

## 1. Introduction

Copper is an essential micronutrient. Many proteins and enzymes, such as cytochrome oxidases, laccases, superoxide dismutases, plastocyanin, or nitrite reductase (Argüello et al., 2013), which are involved in a variety of key biological functions in most living organisms require copper as a redox cofactor (Xu et al., 2021). Nevertheless, the ability to undergo redox reactions makes free copper a potential hazard (Argüello et al., 2013), catalyzing the formation of highly reactive hydroxyl radicals (Gaetke and Chow, 2003). This is particularly relevant when organisms are exposed to high copper concentrations. In such conditions, copper may also attack and destroy iron-sulfur clusters, thereby releasing iron, which can in turn cause further oxidative stress (Rensing and McDevitt, 2013), leading to severe cell damage.

Due to its toxicity in high concentrations, copper can be used to control unwanted microbial growth. This feature has been streamlined in the course of evolution: the innate immune system in mammals utilizes copper intoxication to reduce intracellular survival of bacterial pathogens (Djoko et al., 2015). Besides, several anthropogenic activities also employ copper-based solutions to control microbial biofilm formation, including in medical settings, industrial equipment and plumbing systems (Gomes et al., 2020). Even certain sectors of the agri-food industry, such as grape-wine production (EFSA et al., 2018) and aquaculture (Yanong, 2010) resort to copper-based compounds to tackle fungal and bacterial growth. Despite the toxicity and risk of contamination, copper-based compounds are easy and cheap to obtain, do not discolor the water, and are one of the few effective options for organic growers, which still motivates their use (Romanazzi et al., 2020; Yanong, 2010).

Throughout evolution, bacteria have developed copper-transport systems tightly controlling uptake and secretion, but also trafficking through different compartments, promoting a highly regulated balance of copper metabolism (Argüello et al., 2013; Rensing and McDevitt, 2013). Particularly, when exposed to high copper levels, bacteria have shown to activate several systems that effectively help in copper efflux, reducing its noxious effects intracellularly. In spite of different bacteria exhibiting different combinations of copper-efflux components (Argüello et al., 2013), the two essential mechanisms for copper export rely on: (i), transmembrane-protein complexes that cross the cell wall and pump copper from the cytoplasm, or periplasm in Gram-negative bacteria, directly into the extracellular space; and (ii), export of metallochaperones with copper binding capacity, which can work as chelating agents (Nies, 2003; Argüello et al., 2013; Rensing and McDevitt, 2013). Bacterial cells regulate these processes mainly by modifying transporter abundance through transcriptional control, which also facilitates co-regulation of chaperone and chelating metalloproteins (Argüello et al., 2013).

Similar to higher organisms, bacteria release extracellular vesicles (EVs), which have been shown to play fundamental roles in bacterial cell survival, including secretion, communication, and nutrient uptake (Lima et al., 2020). Many studies on vesicles from Gram-negative bacteria predominantly discuss the classic concept of outer membrane vesicles (OMVs). However, there has been a trend in the past few years to refer generally to vesicles from Gram-negative bacteria as EVs (e.g. Biller et al., 2021; McMillan and Kuehn, 2021; Biller et al., 2022). This is mainly due to the fact that recent studies have shown additional routes for vesicle formation, which are not limited to OMVs (Toyofuku et al., 2019). Thus, in this study, we collectively refer to the vesicles produced by bacteria as EVs.

The Cyanobacteria phylum is a large phylogenetic group of the domain bacteria, with the particular feature of being capable of performing oxygenic photosynthesis with water as an electron donor (Garcia-Pichel et al., 2020), similarly to green algae and plants. These photoautotrophic microorganisms play a key role in the biogeochemical cycle of carbon on a global scale, as estimates predict a global net primary production of 12 gigatonnes each year for marine cyanobacteria only, representing approximately 25% of ocean net primary production (Flombaum et al., 2013). The capacity of cyanobacteria to release EVs was documented in detail for the first time in 2014, and cyanobacterial EVs were proposed to function as vehicles for the movement of carbon through marine food webs, as vectors for horizontal gene transfer, and as decoys for predators and phages (Biller et al., 2014). More recently, the model cyanobacterium *Synechocystis* sp. PCC 6803 (hereafter *Synechocystis*) was also shown to vesiculate (Pardo et al., 2015), and a *Synechocystis* mutant strain, lacking a functional TolC-protein, was described to release substantially more EVs than the parental strain (Oliveira et al., 2016). TolC is an outer membrane protein, essential for the export of proteins (Oliveira et al., 2016; Agarwal et al., 2018; Gonçalves et al., 2018), fatty acids (Bellefleur et al., 2019), and exogenous compounds that reach the cytoplasm (Oliveira et al., 2016; Gonçalves et al., 2018). It was proposed that hypervesiculation in the *Synechocystis tolC*-mutant was a response to the impaired classical secretion (Oliveira et al., 2016). Nevertheless, deletion of inner membrane and periplasmic adaptor components of TolC-dependent efflux systems showed that none of those mutants reached the high vesiculation capacity presented by the *tolC*-deletion mutant (Gonçalves et al., 2018). Thus, it remains to be fully determined why the *Synechocystis tolC*-deletion mutant hypervesiculates.

In this work, we carried out a comprehensive study of the *Synechocystis tolC*-mutant phenotype, in order to clarify why this strain releases more EVs than the wild-type. Combining a quantitative proteomic study with metal resistance tests, intracellular metal quantifications, and biochemical analyses, we show that the *Synechocystis tolC*-mutant accumulates copper intracellularly, uncovering the role of TolC in copper efflux in *Synechocystis*. More importantly, we show that EVs release is a common bacterial response upon exposure to high copper levels, and we detect the presence of a copper-binding chaperone in isolated cyanobacterial EVs. Moreover, detection and quantitation of copper in EVs isolated from the copper-sensitive *Synechocystis tolC*-mutant, cultivated under standard growth conditions, highlights that EVs in bacteria represent an overlooked copper-secretion mechanism. These results contribute to a deeper understanding of the intricate mechanisms warranting copper homeostasis in bacteria, further expanding the role of EVs in bacterial metal metabolism.

## 2. Experimental

### 2.1. Strains and growth conditions

The unicellular cyanobacterium *Synechocystis* sp. PCC 6803 (hereafter *Synechocystis*) wild-type strain and respective mutants used in this work, namely Δ*tolC*, Δ*copB*, Δ*sll1180* (or Δ*hlyB*), Δ*slr1053* (or Δ*acrA*), and EV-trc-GFP (see below) were routinely maintained in BG11 medium (Stanier et al., 1971) supplemented, when necessary, with appropriate antibiotics, in 100 mL Erlenmeyer flasks, with orbital shaking, under a regimen of 12 h light (25 μmol photons $m^{-2}$ $s^{-1}$)/ 12 h dark at 30 ºC. Growth was assessed by measuring optical density at 730 nm ($OD_{730}$). Cyanobacterial strains were routinely streaked on solid BG11 medium

plates to assess the axenic state of the cultures. Unless stated otherwise, *Synechocystis* cells were inoculated at an initial $OD_{730}$ of 0.05 in BG11 and grown in glass gas washing bottles with aeration (approx. 1 L air $min^{-1}$), under a regimen of 16 h light (45 μmol photons $m^{-2}$ $s^{-1}$)/ 8 h dark at 28 ºC, for approximately 3.5 days (unless stated otherwise), reaching a final $OD_{730}$ of approximately 0.8–1.0.

*Escherichia coli* [strain BL21 (DE3)] and *Pseudomonas aeru*ginosa [PAO-1 (ATCC 47085)] were routinely maintained/streaked in LB medium agar plates. Both strains were grown over-night (ON) in 50 mL sterile conical centrifuge tubes, containing 5 mL of liquid LB medium, with orbital shaking (150 rpm for *E. coli*, or 200 rpm for *P. aeruginosa*) at either 37 ºC (*E. coli*) or 30 ºC (*P. aeruginosa*). ON-grown cultures were used to inoculate 200 mL of LB medium, LB supplemented with 0.5, 1 and 2 mM $CuSO_4$ for *E. coli*, or LB supplemented with 1 and 3 mM $CuSO_4$ for *P. aeruginosa*, in 1000 mL Erlenmeyer flasks with an initial $OD_{600}$ of 0.05, at the above-mentioned conditions for 15–16 h, reaching a final $OD_{600}$ of approximately 3.0–5.0.

### 2.2. Proteomics analysis by iTRAQ

The proteomes of *Synechocystis* wild type and *tolC*-mutant were analyzed by 8-plex isobaric tags for relative and absolute quantification (iTRAQ), using four biological replicates. Cultures were grown in BG11 in 500 mL Erlenmeyer flasks, with orbital shaking, under a regimen of continuous light (35 μmol photons $m^{-2}$ $s^{-1}$) at 30 ºC. Upon reaching an $OD_{730}$ of approximately 1.0–1.5, cells were collected by centrifugation (4400 *g*, at room temperature), washed with potassium phosphate buffer (50 mM $K_2HPO_4$, 50 mM $KH_2PO_4$, pH 6.9) and stored at − 80 ºC until further analysis. A detailed description of protein extraction and analysis can be found in the Supporting information file (**Text S1**).

### 2.3. Synechocystis metal resistance analysis

To evaluate the metal resistance capacity of *Synechocystis* wild-type and mutant strains, cells were grown in solid BG11 (lacking sodium thiosulfate) supplemented with different metals, namely boron (463 μM $H_3BO_3$), cadmium (5 μM $CdN_2O_6.4\ H_2O$), cobalt (5 μM Co $(NO_3)_2.6\ H_2O$), copper (4 μM $CuSO_4$), iron (229 μM Ferric ammonium citrate), manganese (91.5 μM $MnCl_2.4\ H_2O$), molybdenum (16.1 μM $Na_2MoO_4.2\ H_2O$), nickel (7 μM $NiSO_4.6\ H_2O$), or zinc (14 μM $ZnSO_4$). *Synechocystis* cultures were grown as indicated in "*Strains and growth conditions*". Later, cells were harvested by centrifugation (4400 *g*, 10 min at room temperature) and the cell pellet was suspended in fresh liquid BG11 medium, to a final $OD_{730}$ of 10. Serial dilutions were then prepared, and 15 μL of each cell suspension were spotted onto solid BG11 supplemented with each metal. Petri dishes were incubated for 7 days, under a regimen of 16 h light (25 μmol photons $m^{-2}$ $s^{-1}$)/8 h dark at 28 ºC, and cell growth was registered by photographing the dishes. To quantify growth differences, a densitometry analysis was carried out using ImageJ (Schneider et al., 2012).

### 2.4. Intracellular metal quantification by atomic absorption spectrometry

The intracellular levels of cobalt, copper, iron and zinc in *Synechocystis* wild-type and *tolC*-mutant strain were quantified by atomic absorption spectrometry (AAS). Briefly, cells were cultivated as described above and collected at an $OD_{730}$ of 0.8–1.0. Then, cells were pelleted by centrifugation at 4400 *g* for 10 min, and thoroughly washed using extraction buffer (20 mM Tris-HCl, 5 mM EDTA, pH 8.0). Later, cells were transferred to a screw-capped, 2 mL microcentrifuge tube, collected by centrifugation at 16,000 *g* for 1 min at 4 ºC, and washed twice again with extraction buffer for complete removal of BG11 traces. Finally, cell pellets were mixed with 100 μL of 65% $HNO_3$, and incubated at 75 ºC for 12 min, vigorously vortexed every 2 min. Following this procedure, 1 mL of Milli-Q® Type 1 Ultrapure water was added, samples mildly vortexed, and centrifuged at 16,000 *g* for 5 min at room temperature. The resulting supernatant was collected for AAS analyses. Copper, iron and zinc levels were determined with an atomic absorption spectrometer coupled to a flame atomization detector (Perkin Elmer), while cobalt levels were determined with a spectrometer with an electrothermal detector (Perkin Elmer). For the various metals, quantifications were performed against calibration curves using specific aqueous pattern solutions. Results are presented in μg of metal $L^{-1}$ culture $OD_{730}{}^{-1}$.

### 2.5. Total RNA extraction and analysis of transcript levels by RT-qPCR

Sample collection, RNA extraction, all the control measurements and PCRs were performed as previously described (Gonçalves et al., 2018). For cDNA synthesis, 5 μg of total RNA was transcribed with the iScriptTM Advanced cDNA Synthesis Kit for RT-qPCR (Bio-Rad) in a final volume of 20 μL, following the manufacturer's instructions. A control PCR was performed using 1 μL of cDNA as template in reaction mixtures containing: 0.5 U of GoTaq® G2 Flexi DNA Polymerase (Promega), 1x Green GoTaq Flexi buffer, 200 μM of each dNTP, 1.5 mM $MgCl_2$, 0.25 μM of each *rnpB* primer (Table S1). For the determination of the primers' efficiency, three-fold standard dilutions of the cDNAs were made (1/3, 1/9, 1/27, 1/81 and 1/243) and stored at − 20 °C. RT-qPCRs were performed on Hard-Shell 384-Well PCR Plates (thin wall, skirted, clear/white) covered with Microseal® B adhesive seal (Bio-Rad). Ten microliter reactions were manually assembled and contained: 0.25 μM of each primer (Table S1), 5 μL of iTaq™ Universal SYBR® Green Supermix (Bio-Rad) and 1 μL of template cDNA (dilution 1/9). The PCR profile was: 3 min at 95 °C followed by 45 cycles of 30 s at 95 °C and 30 s at 60 °C; and in the end a melting curve analysis (10 s cycles between 55 and 95 °C with a 0.5 °C increment per cycle). Primer efficiency standard curves and negative controls (no template cDNA) were included in all assays. RT-qPCRs were performed with three biological replicates and technical triplicates of each cDNA sample in the CFX384 Touch™ Real-Time PCR Detection System (Bio-Rad). The normalized expression of the target genes was calculated using the Bio-Rad CFX Maestro™ 3.1 software (Bio-Rad), implementing an efficiency-corrected delta-delta Cq method (ΔΔCq). Statistical analysis was performed by means of a one-way ANOVA using the same software, and tests were considered significant if $P < 0.05$. Genes *bfrA*, *sll0083* and *slr0769* were validated as reference genes for data normalization (M value < 0.5), using the reference gene selection tool available in the Maestro™ software. The size of the PCR products for each gene was checked by agarose gel electrophoresis performed by standard protocols. These products were also cloned into the pGEM-T® Easy (Promega) vector according to the manufacturer's instructions. Identity of the amplicons was confirmed by Sanger sequencing (StabVida). These experiments were compliant with the MIQE guidelines (Bustin et al., 2009) to promote the effort for experimental consistency and transparency, and to increase the reliability and integrity of the results obtained.

### 2.6. Generation of the Synechocystis strain producing sfGFP-loaded EVs

To construct the *Synechocystis* strain expressing the heterologous protein sfGFP and further targeting it to EVs, the synthetic promoter $P_{trc.x.lacO}$ (Ferreira et al., 2018), the signal peptide sequence of the *Synechocystis* native protein FutA2 (Polyviou et al., 2018), which determines its translocation to the periplasm, and the gene encoding the reporter protein super-folder Green Fluorescent Protein (sfGFP) were amplified by PCR using specific oligonucleotides (Table S1). Assembly of the different DNA fragments was performed by sequential overlap-extension PCR. The 953 bp fragment was digested with *Pst*I and *Xba*I, and ligated to plasmid pSN15KPO previously digested with the same restriction enzymes, rendering plasmid pEV-trc-GFP. Identity of the fragment was determined by Sanger sequencing. Plasmid pSN15KPO is a variant of plasmid pSN15K (Pinto et al., 2015), in which the kanamycin resistance cassette was replaced by that of plasmid pUC4K (GE

Healthcare). *Synechocystis* wild-type cells were naturally transformed with pEV-trc-GFP, and fully segregated mutants were obtained, rendering strain EV-trc-GFP.

### 2.7. Total protein extraction, concentration of cell-free extracellular medium and protein analyses

Cells from *Synechocystis* wild-type and mutant strains were grown as described above, and harvested by centrifugation at 4400 *g* for 10 min at room temperature. Total protein extracts were obtained as described (Lopes Pinto et al., 2011). In brief, cell pellets were suspended in protein extraction buffer [10 mM HEPES, 0.5% (v/v) Triton X-100, 10 mM EDTA, 2 mM DTT, 10% (v/v) glycerol, pH 8.0, supplemented with protease inhibitor cocktail (Roche)] and disrupted by sonication (Branson Sonifier 250). Subsequently, samples were centrifuged at 10, 000 *g* for 10 min at 4 °C, and the resulting supernatant transferred into a new 1.5 mL microcentrifuge tube and stored at − 20 ºC until further analysis. Protein concentration was determined using the BCA method (Thermo Fisher Scientific), with bovine serum albumin as standard. For cell-free, extracellular medium concentrated samples, the method described by Oliveira et al. (2015) was followed. Briefly, cells were cultivated as described up to an $OD_{730}$ of approximately 1.0–1.5, and later separated from the extracellular medium by centrifugation (4400 *g*, 10 min at room temperature). Spent medium was filtered through 0.2 μm pore size filters for cell removal, and further concentrated approximately 1000-fold by ultrafiltration, using Amicon® Ultra-15 Centrifugal Filter Units (Merck) with molecular weight cut-off of 3 kDa. Concentrated samples were either used immediately or stored at − 20 ºC. The amount of concentrated spent medium sample analyzed was normalized by cell culture density ($OD_{730}$), volume of cell-free culture medium concentrated, and concentration factor. Total protein and cell-free, concentrated extracellular medium samples were electrophoresed on homogeneous 12 or 16% (w/v) SDS polyacrylamide gels, stained with colloidal Coomassie Brilliant Blue (Sigma), and gels were scanned with a GS-800 Calibrated Densitometer (BioRad).

For Western blotting, after SDS-polyacrylamide gel electrophoresis, protein samples were transferred onto a nitrocellulose membrane (GE Healthcare). Membranes were incubated in Blocking buffer [5% (w/v) fat-free milk powder, and 0.05% (v/v) Tween-20 in TBS (20 mM Tris-base, 0.8% (w/v) NaCl, pH 7.6)] for 2 h before being incubated overnight at 4 ºC with rabbit anti-CopM antibody (Giner-Lamia et al., 2015) (1:3000) in fresh blocking buffer. After incubation with the primary antibody, membranes were washed twice in TTBS [0.05% (v/v) Tween-20 in TBS], incubated for 1 h with an anti-rabbit secondary antibody conjugated with horseradish peroxidase (Sigma) (1:10000), washed again twice with TTBS and twice with TBS. For sfGFP detection, the commercial mouse anti-GFP monoclonal antibody (Roche) (1:5000), and the goat-anti-mouse secondary antibody (Invitrogen) (1:5000) were used. Detection was carried out on a ChemiDoc MP System (BioRad), using the Clarity™ Western ECL Substrate (BioRad) reagent according to the manufacturer's instructions.

### 2.8. Extracellular vesicles isolation and analysis

*Synechocystis* cultures were grown as presented above ("Strains and growth conditions") and extracellular vesicles (EVs) were isolated as follows: cyanobacterial cells were separated from the extracellular medium by centrifugation at 4400 *g* for 10 min at room temperature, and further removed from the extracellular medium by filtration (0.2 μm filter pore size). Cell-free extracellular medium was then concentrated by ultrafiltration (4400 *g*, 16 °C) using Amicon® Ultra-15 Centrifugal Filter Units (Merck) with a molecular weight cut-off of 100 kDa. Later, concentrated samples were diluted with 15 mL of fresh BG11 medium and ultracentrifuged (70 Ti fixed angle rotor, Beckman Coulter Optima L80 XP Ultracentrifuge) using polycarbonate bottles with cap assembly (#355618) for 3 h at 100,000 *g* at 4 °C. Finally, the resulting pellet was suspended in sterile BG11 growth medium, and stored at − 80 ºC until further analysis.

*E. coli* cultures were grown as described, and EVs isolated similarly as performed for *Synechocystis* EVs. Briefly, cells were collected by centrifugation at 4400 *g* for 15 min at room temperature, and further removed from the extracellular medium by filtration (0.45 μm filter pore size). Then, cell-free extracellular medium was concentrated by ultrafiltration (4400 *g*, 4 °C) with centrifugal filters with a molecular weight cut-off of 100 kDa (Pall). Prior to ultracentrifugation, samples were mixed with 15 mL of PBS (Phosphate Buffered Saline, 1X, pH 7.5) and filtered once again (0.45 μm) to ensure complete removal of any biological contaminant. Ultracentrifugation was performed for 2 h at 174,900 *g* (70 Ti fixed angle rotor, Beckman Coulter Optima L80 XP Ultracentrifuge) at 4 °C. The resulting pellet was suspended in sterile PBS, and stored at − 80 ºC until further analysis.

A similar procedure was performed to isolate EVs from *P. aeruginosa*. Cells were collected by centrifugation at 10,000 *g* for 30 min at room temperature, and further removed from the extracellular medium by filtration (0.45 μm filter pore size). Then, cell-free extracellular medium was also concentrated by ultrafiltration (4400 *g*, 4 °C). Prior to ultracentrifugation, samples were treated as mentioned: washed with 15 mL of PBS and filtered once again (0.45 μm). Ultracentrifugation was performed for 3 h at 150,000 *g* at 4 °C. The resulting pellet was suspended in sterile PBS, and stored at − 80 ºC until further analysis.

Various methodologies were performed to evaluate EVs physical features and biochemical composition. Briefly, EVs number and size were analyzed by nanoparticle tracking analysis and their morphological aspect by electron microscopy. Regarding EVs composition, proteins and lipopolysaccharides (LPS) were routinely analyzed by SDS-polyacrylamide gel electrophoresis. Detection of CopM in isolated *Synechocystis* EVs was carried out by Western blot, and vesicular copper levels were quantified by atomic absorption spectrometry (AAS) (see further details about these techniques in Supporting information **Text S1**).

## 3. Results

### 3.1. Inactivation of the TolC-like protein in Synechocystis results in several adaptations at the protein level

The TolC-like protein (Slr1270) has been shown in *Synechocystis* to play key roles in protein export and multidrug efflux (Oliveira et al., 2016) as part of the type I secretion system (T1SS) and of the resistance-nodulation-division (RND) efflux pumps (Gonçalves et al., 2018). In addition, a *Synechocystis tolC*-mutant strain was shown to release more EVs than the respective wild-type (Oliveira et al., 2016; Gonçalves et al., 2018). In order to get closer insights into the adaptations occurring in *Synechocystis* cells lacking a functional TolC-like protein, iTRAQ-based quantitative shotgun proteomics was carried out. In this study, a total of 1135 proteins were identified with quantification information [with at least two peptides, and at a false discovery rate (FDR) of less than 1%], corresponding to approximately 32.4% of the total predicted *Synechocystis* proteome. 212 proteins were found to be differentially expressed between the strains analyzed (Table S2). Among the statistically significant differentially expressed proteins, 46 show at least 1.35-fold up- or down-regulation in respect to wild-type protein levels (Table 1), with more than 35% of the hits falling in the "hypothetical" or "functionally uncharacterized" protein categories. Some of the proteins differentially expressed have been previously reported to accumulate differently in the *tolC*-mutant strain as compared to the wild-type, namely proteins Sll1951 (−3.25-fold), Slr1841 (1.38-fold), and ApcE (1.41-fold) (Oliveira et al., 2016). In addition, proteins related to metal uptake and homeostasis, particularly CopM-Slr6039/Sll0788 (1.75-fold), FutA1 (1.43-fold), FrpC (−2.06-fold), or whose function is dependent on metal cofactors, namely IsiB (3.18-fold) and cytochrome $c_6$ (−2.55-fold), were found amongst

**Table 1**
List of proteins identified in the iTRAQ (isobaric tags for relative and absolute quantification) proteomics analysis with differential accumulation (> 1.35-fold; < −1.35-fold) in the *Synechocystis* sp. PCC 6803 *tolC*-mutant strain in respect to the wild-type strain cultivated under standard growth conditions.

| Uniprot | # peptides | Protein names | Gene names | Fold Changes |
|---|---|---|---|---|
| P27319 | 22 | Flavodoxin | *isiB* sll0248 | **3.18** |
| P73742 | 100 | Sll0858 protein | sll0858 | **2.95** |
| P73238 | 31 | Slr2018 protein | slr2018 | **2.18** |
| P73354 | 28 | Serine protease HtrA | *htrA* slr1204 | **2.08** |
| Q6YRW5 | 2 | Slr6039 protein | slr6039 | **1.75** |
| P72656 | 2 | Ribonuclease E/G-like protein | *rne* slr1129 | **1.75** |
| Q55604 | 3 | Slr0769 protein | slr0769 | **1.69** |
| P73066 | 29 | Ycf23 protein | *ycf23* slr2032 | **1.46** |
| Q55665 | 58 | Glutamate-1-semialdehyde 2,1-aminomutase (GSA) | *hemL gsa* sll0017 | **1.44** |
| P72827 | 21 | Iron uptake protein A1 | *futA1* slr1295 | **1.43** |
| P73315 | 20 | 50 S ribosomal protein L22 | *rplV rpl22* sll1803 | **1.43** |
| P74791 | 6 | PirA (PII interacting protein A) | ssr0692 | **1.42** |
| P37101 | 163 | Phosphoribulokinase (PRK) | *prk ptk* sll1525 | **1.41** |
| Q55544 | 60 | Phycobiliprotein ApcE | *apcE* slr0335 | **1.41** |
| P74786 | 6 | UPF0426 protein ssl0294 | ssl0294 | **1.39** |
| P72851 | 9 | 50 S ribosomal protein L28 | *rpmB* rpl28 *ssr1604* | **1.38** |
| Q55797 | 14 | Phosphoheptose isomerase (EC 5.3.1.28) (Sedoheptulose 7-phosphate isomerase) | *gmhA* sll0083 | **1.38** |
| P73409 | 9 | Slr1841 protein | slr1841 | **1.38** |
| P74478 | 16 | Slr1926 protein | slr1926 | **1.38** |
| P73288 | 40 | Aklaviketone reductase | sll1825 | **1.35** |
| P73644 | 6 | S-adenosyl-methionine: precorrin-2 methyltransferase | *cbiL* | **-1.35** |
| Q55770 | 40 | Sll0185 protein | sll0185 | **-1.36** |
| P52981 | 22 | 1,4-alpha-glucan branching enzyme GlgB | *glgB* sll0158 | **-1.36** |
| P74722 | 3 | Slr0586 protein | slr0586 | **-1.36** |
| P37277 | 6 | Photosystem I reaction center subunit XI (PSI subunit V) (PSI-L) | *psaL* slr1655 | **-1.36** |
| Q55146 | 9 | Sll0064 protein | sll0064 | **-1.37** |
| Q55162 | 10 | Sll0051 protein | sll0051 | **-1.38** |
| Q55961 | 8 | Slr0699 protein | slr0699 | **-1.39** |
| P73111 | 19 | Sll1835 protein | sll1835 | **-1.39** |
| P73477 | 7 | Slr1232 protein | slr1232 | **-1.42** |
| P74748 | 10 | Slr0602 protein | slr0602 | **-1.42** |
| P73595 | 59 | Uncharacterized WD repeat-containing protein slr1410 | slr1410 | **-1.42** |
| Q55735 | 3 | Sll0394 protein | sll0394 | **-1.44** |
| P73559 | 7 | Slr0878 protein | slr0878 | **-1.45** |
| P73594 | 62 | Uncharacterized WD repeat-containing protein slr1409 | slr1409 | **-1.46** |
| Q55561 | 10 | Sll0167 protein | sll0167 | **-1.46** |
| P73731 | 5 | Photosystem II reaction center Psb28 protein | slr1739 | **-1.46** |
| P74485 | 15 | Sll1863 protein | sll1863 | **-1.52** |
| P74486 | 2 | Sll1862 protein | sll1862 | **-1.54** |
| Q55549 | 2 | Slr0168 protein | slr0168 | **-1.54** |
| P74162 | 24 | Sll1380 protein | sll1380 | **-1.70** |
| Q55776 | 9 | Sll0180 protein | sll0180 | **-1.79** |
| P73019 | 5 | Iron-regulated protein | *frpC* sll1009 | **-2.06** |
| P46445 | 14 | Cytochrome $c_6$ | *petJ* sll1796 | **-2.55** |
| Q55747 | 42 | Slr0420 protein | slr0420 | **-2.64** |
| P73817 | 13 | Hemolysin | sll1951 | **-3.25** |

the most differentially expressed proteins.

### 3.2. TolC is essential for metal homeostasis in Synechocystis

Based on these proteomic results, we wondered whether the *tolC*-mutant could be under some sort of metal imbalance. To address this question, the growth of the cyanobacterial strains was tested in the presence of selected metals, namely boron, cadmium, cobalt, copper, iron, manganese, molybdenum, nickel, and zinc (Fig. 1A). No differences in growth could be observed between *Synechocystis* wild-type and *tolC*-mutant in medium supplemented with boron, cadmium, manganese, molybdenum, or nickel. In contrast, significant growth impairment was detected in the mutant strain cultivated in medium supplemented with copper and zinc, and, to a lesser extent, cobalt and iron, when compared to the wild-type. Therefore, we proceeded to determine the intracellular levels of cobalt, copper, iron and zinc by atomic absorption spectrometry in both strains cultivated under standard growth conditions (Figs. 1B and S1). While similar intracellular levels for cobalt, iron and zinc could be detected in both strains (Fig. S1), *tolC*-mutant cells were found to accumulate approximately 3-fold more copper than the wild-type (Fig. 1B).

At this point, we hypothesized that the role of TolC in copper homeostasis could be related to: (i) the export of an unknown protein with copper-binding ability, via the T1SS; (ii) the efflux of copper through an RND pump; or (iii) the efflux of copper through a heavy metal efflux (HME) pump. To address these possibilities, we cultivated *Synechocystis* wild-type, and mutant strains Δ*tolC*, Δ*hlyB* (lacking the inner membrane component of the T1SS (Gonçalves et al., 2018)), Δ*acrA* (lacking the periplasmic adaptor protein of the main RND pump in *Synechocystis* (Gonçalves et al., 2018)), and Δ*copB* (mutant lacking the periplasmic adaptor protein of the copper-specific HME-pump in *Synechocystis* (Giner-Lamia et al., 2012)) in medium supplemented with copper, and the growth of the various strains was analyzed (Fig. 2). All strains grew similarly under standard growth conditions (0.5 μM $Cu^{2+}$), and cells of the *acrA*-mutant strain presented the same growth capacity as the wild-type strain when cultivated in medium supplemented with copper (4.0 μM $Cu^{2+}$). However, while cells of the *hlyB*-mutant could grow slightly better than those of the wild-type strain under copper-challenging conditions, both the *copB*- and *tolC*-mutant strains exhibited growth impairment when compared to the wild-type. Remarkably, the *tolC*-mutant showed a more severe growth impairment as compared to the *copB*-mutant (Fig. 2).

Altogether, these observations suggest that TolC plays a key role in metal homeostasis in *Synechocystis*, particularly in keeping an intracellular balance of copper levels, likely working as the outer membrane component of the HME-pump dedicated to copper export.

### 3.3. Absence of TolC in Synechocystis triggers upregulation of copper detoxification mechanisms

Two main mechanisms have been described in *Synechocystis* to warrant copper detoxification, both being involved in metal export when cells are challenged with stressfully high copper concentrations: the HME-pump (dependent on the CopBA system), and the periplasmic metallochaperone system (dependent on CopM). In order to evaluate how these systems responded in the *Synechocystis tolC*-mutant strain, Western blotting experiments and/or transcriptional analyses were carried out. On one hand, RT-qPCR experiments revealed that the *tolC*-mutant has significantly higher *copB* transcript levels than the wild-type (Fig. 3A). On the other hand, transcript analysis by Northern blotting showed that the *tolC*-mutant accumulates higher levels of *copM* transcripts than the wild-type (data not shown). In agreement, iTRAQ results (Table 1) also indicated that CopM (Slr6039/Sll0788) is significantly overexpressed in *tolC*-mutant cells. Using a CopM-specific antibody (Giner-Lamia et al., 2015), Western blotting experiments determined that the intracellular CopM levels in the *tolC*-mutant strain are

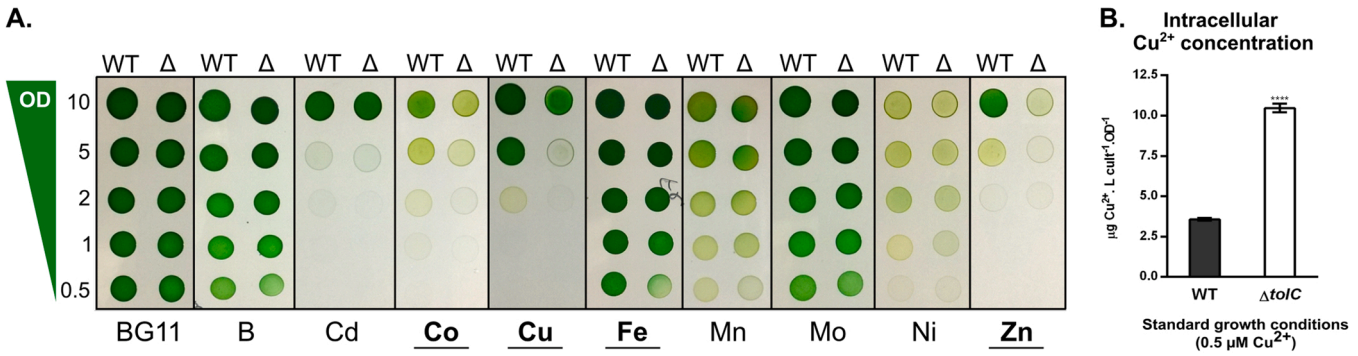


**Fig. 1.** The *Synechocystis* sp. PCC 6803 *tolC*-mutant shows a growth-sensitive phenotype when cultivated in the presence of elevated concentrations of specific metals. A. Cells of *Synechocystis* wild-type (WT) and *tolC*-mutant (Δ) strains were cultivated in standard liquid conditions up to an $OD_{730}$ of approximately 0.8–1.0, concentrated to an $OD_{730}$ of 10, and later diluted ($OD_{730}$ of 5, 2, 1, 0.5). Cells of each dilution were spotted onto standard BG11 agar plates (BG11), or BG11 agar plates supplemented with boron (B - 463 μM), cadmium (Cd - 5 μM), cobalt (Co - 5 μM), copper (Cu - 4 μM), iron (Fe - 229 μM), manganese (Mn – 91.5 μM), molybdenum (Mo - 16.1 μM), nickel (Ni - 7 μM), or zinc (Zn - 14 μM), and cultivated for 7 days. Presented photographs are representative of the results obtained with 3 independent biological replicates. Bold and underlined metal symbols indicate conditions in which the *Synechocystis tolC*-mutant showed growth-sensitive phenotype when compared to the wild-type strain, and further selected for intracellular quantification of the respective metal's concentration. **B.** Intracellular copper concentration determined for *Synechocystis* wild-type (WT) and *tolC*-mutant (Δ*tolC*) strains cultivated under standard liquid BG11 conditions. Copper levels were determined by atomic absorption spectrometry, and are shown in μg $Cu^{2+}$.L $culture^{-1}$.$OD_{730}{}^{-1}$. Error bars represent the standard deviations of at least three independent biological replicates. ****, $P \leq 0.0001$.

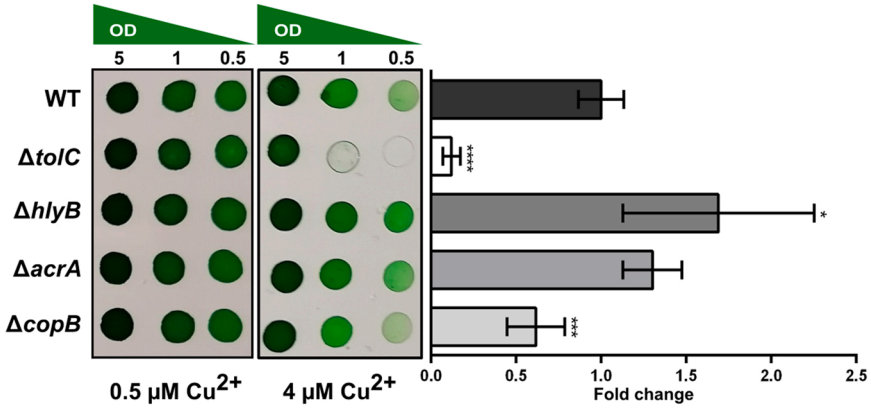


**Fig. 2.** The *Synechocystis* sp. PCC 6803 *tolC*-mutant copper-sensitive phenotype is not associated to its T1SS- or to its RND-dependent function. Cells of *Synechocystis* wild-type (WT), and mutant strains Δ*tolC*, Δ*hlyB* (T1SS), Δ*acrA* (RND), Δ*copB* (HME-pump) were cultivated in standard liquid conditions up to an $OD_{730}$ of approximately 0.8–1.0, concentrated to an $OD_{730}$ of 5, and later diluted ($OD_{730}$ of 1 and 0.5). Cells of each dilution were spotted onto standard BG11 agar plates (0.5 μM $Cu^{2+}$), or BG11 agar plates supplemented with copper (4 μM $Cu^{2+}$), and cultivated for 7 d. Presented photographs are representative of the results obtained with 3 independent biological replicates. The panel to the right shows cell density quantification by densitometry analysis (Image J) determined for each cyanobacterial strain, spotted at initial $OD_{730}$ of 0.5, and cultivated in BG11 agar plates supplemented up to a final concentration of 4 μM copper sulfate. Error bars represent the standard deviations of at least three independent biological replicates. *, $P \leq 0.05$; ***, $P \leq 0.001$; ****, $P \leq 0.0001$, each determined against the WT.

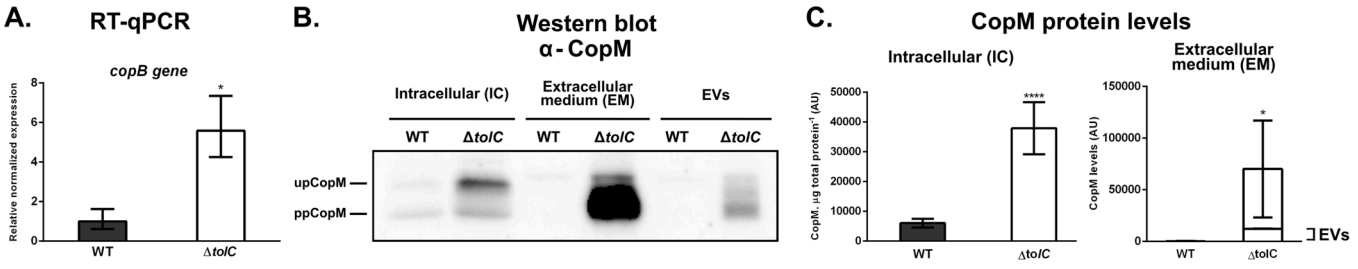


**Fig. 3.** *Synechocystis* sp. PCC 6803 *tolC*-mutant shows high upregulation of the copper detoxification mechanisms under standard growth conditions. A. RT-qPCR analysis of the *copB* transcript levels in *Synechocystis* wild-type (WT) and *tolC*-mutant (Δ*tolC*) strains cultivated under standard growth conditions. B. Western blot analysis of the CopM-protein levels in: 10 μg of total protein extracts (Intracellular - IC); cell-free, concentrated extracellular medium (Extracellular medium - EM); and isolated extracellular vesicles (EVs), of *Synechocystis* wild-type and *tolC*-mutant strains cultivated under standard growth conditions. Concentrated extracellular medium and EVs samples were normalized before loading for initial cell-free culture volume concentrated, final volume of concentrated sample, and culture's $OD_{730}$. upCopM: unprocessed CopM-protein; ppCopM: processed CopM-protein. C. Quantification of CopM protein levels detected by Western blotting in total protein extracts (Intracellular - IC), and in the cell-free extracellular growth medium (Extracellular medium - EM), as determined by densitometry analysis (ImageJ). Contribution of EVs for CopM levels detected in the complete cell-free extracellular medium is highlighted in the graph. Error bars represent the standard deviations of at least three independent biological replicates. *, $P \leq 0.05$; ****, $P \leq 0.0001$.

approximately 6-fold higher than those detected in the wild-type (Fig. 3B and C). Moreover, the two previously described CopM forms could be detected (Fig. 3B): the unprocessed, full-length protein, and the processed CopM, resulting from the signal peptide removal from its N-terminus upon translocation from the cytoplasm to the periplasm (Giner-Lamia et al., 2015). CopM has been described as a periplasmic copper-binding chaperone, but it has also been found to accumulate in the extracellular medium (Giner-Lamia et al., 2015). Accordingly, CopM could also be detected here in cell-free, concentrated extracellular medium samples obtained from both strains, even though in significantly higher amounts in the mutant (Fig. 3B and C). These results suggest that both copper-detoxification mechanisms are activated, and are highly expressed in a *Synechocystis* strain lacking a functional TolC-protein.

### 3.4. The copper-binding chaperone CopM can be found in EVs isolated from Synechocystis

After finding high levels of CopM in extracellular medium samples, it became important to determine whether CopM could be detected in *Synechocystis* EVs. To that end, extracellular medium of both *Synechocystis* wild-type and *tolC*-mutant strain were concentrated by ultrafiltration, and their respective EVs isolated by ultracentrifugation. Western blotting confirmed the presence of CopM protein in EVs, particularly in those isolated from the *tolC*-mutant (Fig. 3B). When normalizing the amount of CopM detected in EVs isolated from wild-type and mutant strain, by the total amount of vesicles recovered in each respective condition as determined by the amount of LPS (molecular marker of EVs released by Gram-negative bacteria), we could estimate that the CopM protein levels are approximately 4-fold higher in *tolC*-mutant EVs as compared to wild-type. Yet, the amount of CopM identified therein corresponded just to a fraction of the total extracellular CopM pool (Fig. 3C).

To investigate if proteins reaching the periplasm of Cyanobacteria could be detected freely available in the growth medium as well as in EVs, we generated a *Synechocystis* mutant expressing the heterologous reporter protein sfGFP (Fig. 4). The gene encoding sfGFP was fused with the Tat-dependent, signal peptide described in the *Synechocystis* periplasmic protein FutA2 (Polyviou et al., 2018), and its expression was controlled by the $P_{trc.x.lacO}$ promoter (Ferreira et al., 2018). Confocal microscopy analysis of transformed cells clearly indicated accumulation of sfGFP-protein in the outermost region of the cell, indicating successful targeting of the reporter to the periplasm (Fig. 4A). Moreover, confocal microscopy also showed that sfGFP is packaged in isolated EVs (Fig. 4B). In agreement, Western blotting analyses of isolated EVs confirmed the presence of sfGFP therein, as well as freely available in EVs-free, concentrated extracellular medium (data not shown). The amount of sfGFP freely available in the medium was close to 8-fold higher than that found in EVs (Fig. 4C). This experiment has now elucidated that soluble proteins reaching the *Synechocystis* periplasm may leave the cell by translocation across the outer membrane or by packaging into EVs, supporting the possibility of CopM being exported by the *Synechocystis* cell by both systems. Moreover, it is also possible that EV-protein cargo is released into the extracellular space by vesicle leakage or breakdown.

### 3.5. Synechocystis wild-type strain produces more CopM-loaded EVs when cultivated in high copper concentrations

In light of these results, the hypervesiculating phenotype observed in the *Synechocystis tolC*-mutant strain could be partly interpreted as a mechanism responding to an intracellular copper accumulation. To evaluate how the *Synechocystis* wild-type strain responded in terms of EVs' production when challenged to grow in the presence of high amounts of copper, the cyanobacterium was cultivated under increasing concentrations of the metal, and the total amount of released EVs was monitored (Figs. 5 and S2). All evidence combined suggests that *Synechocystis* wild-type cells indeed produce more EVs when exposed to high copper concentrations, a response that seems to follow a copper concentration-dependent manner. Interestingly, while regular increments in $Cu^{2+}$ concentration up to 3 μM resulted in modest, but steady increase of EVs' production [as determined by the amount of LPS (Fig. 5A and B) and nanoparticles (Fig. S2)], presence of 4 μM of $Cu^{2+}$ in the medium resulted in a strong boost in vesicle production. In addition, presence of CopM in isolated EVs was also investigated by Western blot: in agreement with the increase in EVs production, the results indicate that the amount of CopM also increases (Fig. 5A). Moreover, detailed analysis of the LPS band profile indicates that EVs released by *Synechocystis* cells challenged with 4 μM of $Cu^{2+}$ present a 5-fold decrease in the amount of high molecular weight, smooth-type LPS relative to the low molecular weight, rough-type LPS (Fig. 5C). This significant difference was also detected in EVs isolated from the *Synechocystis tolC*-mutant strain, though to a lesser extent (Fig. 5C).

### 3.6. Other model Gram-negative bacteria also release EVs when cultivated in the presence of high copper concentrations

Next, we decided to analyze whether this EVs production phenotype in response to growth-challenging copper concentrations was exclusive of Cyanobacteria or if it could also be observed for other Gram-negative bacteria. Thus, similar experiments as described for *Synechocystis* wild-type were carried out for the enteric *Escherichia coli* [strain BL21 (DE3)], and for the opportunistic pathogen *Pseudomonas aeruginosa* (strain PAO-1). EVs production followed a similar pattern as that observed for *Synechocystis* wild-type, i.e. as copper-concentration in the medium increased, the amount of produced vesicles increased as well

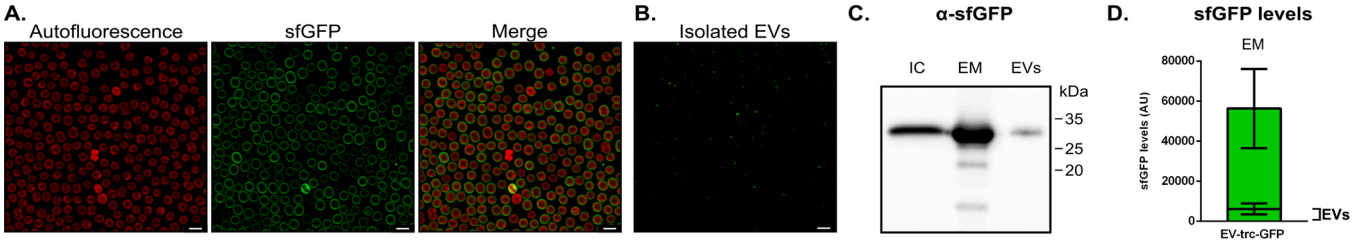


**Fig. 4.** sfGFP translocated to the *Synechocystis* sp. PCC 6803 periplasm can also be detected in the extracellular medium, both as free protein and in extracellular vesicles. A. Confocal micrographs of EV-trc-GFP cells (*Synechocystis* cells expressing sfGFP fused with the signal peptide of the protein FutA2, and under the control of the $P_{trc.x.lacO}$ synthetic promoter) depicting the red autofluorescence signal from the cells' photosynthetic pigments, and the green signal from the sfGFP reporter. A panel showing the result of merging the two micrographs is also presented. Scale bar: 5 μm. B. Confocal micrograph showing green fluorescent foci obtained from EVs isolated from EV-trc-GFP cells. Scale bar: 3 μm. C. Western blot analysis of sfGFP protein in 10 μg of total protein (IC - intracellular), in cell-free concentrated extracellular media (EM) and isolated extracellular vesicles (EVs) samples of EV-trc-GFP cells. EM and EVs samples were normalized for initial cell-free culture volume concentrated, final volume of concentrated sample, and culture's $OD_{730}$. D. Quantification of sfGFP protein levels detected by Western blotting in the complete cell-free extracellular growth medium (EM), and in EVs only, as determined by densitometry analysis (ImageJ). Error bar represents the standard deviation of at least three independent biological replicates.

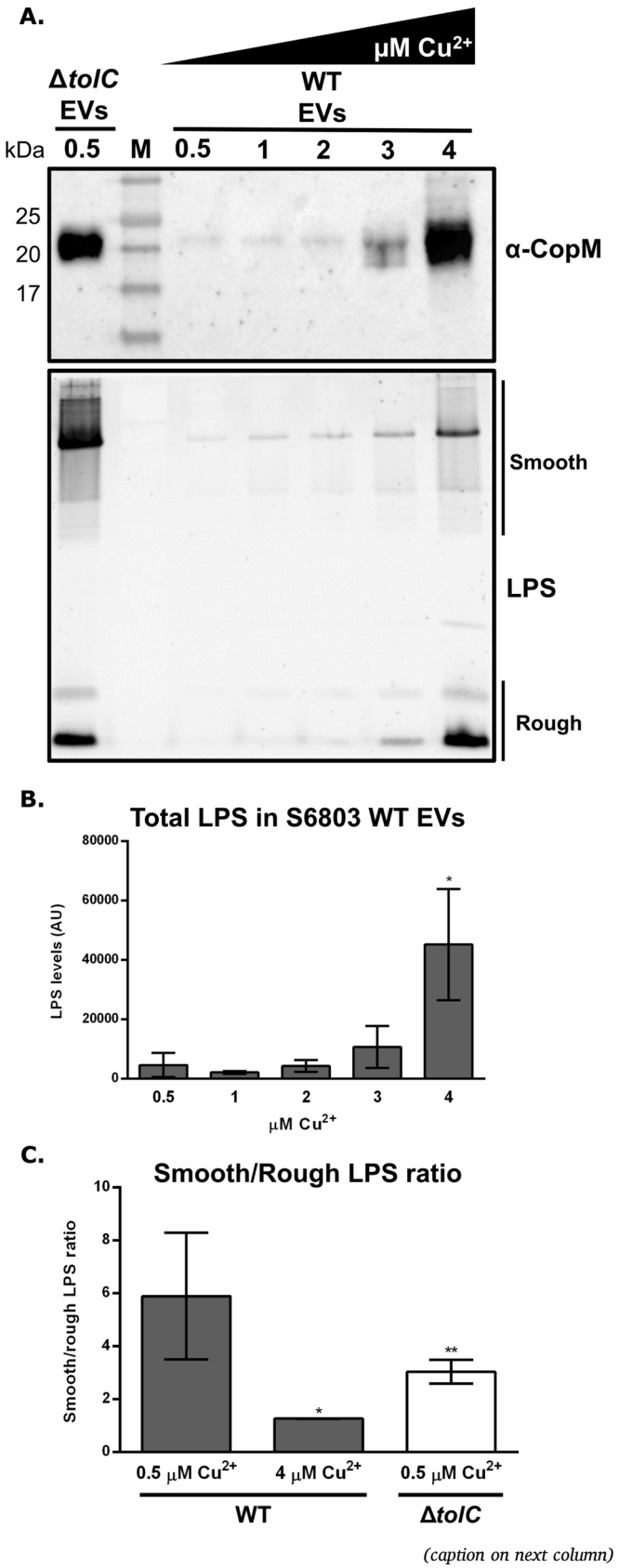


*(caption on next column)*

**Fig. 5.** *Synechocystis* sp. PCC 6803 wild-type produces extracellular vesicles in response to copper supplementation in the medium in a concentration dependent manner. *Synechocystis* wild-type (WT) cells were grown under standard growth conditions (liquid BG11 medium with 0.5 μM $Cu^{2+}$), and later distributed into BG11 standard medium (0.5 μM $Cu^{2+}$) or BG11 medium supplemented with copper to a final concentration of 1, 2, 3 and 4 μM $Cu^{2+}$. In addition, *Synechocystis tolC*-mutant cells (Δ*tolC*) were cultivated in standard conditions, and then further grown in fresh BG11 medium. For all conditions, cyanobacterial cells were cultivated for approximately 7 d, and their respective extracellular vesicles (EVs) isolated. A. Isolated EVs were analyzed by Western blotting for the detection of CopM-protein levels (upper panel). M, NZYColour Protein Marker II ladder (NZYTech). Molecular weight of selected bands is shown to the left in kDa. As lipopolysaccharides (LPS) are regarded as a marker for the presence and abundance of Gram-negative EVs, EVs samples were separated by electrophoresis on 16% (w/v) SDS-polyacrylamide gels and LPS were stained using the Pro-Q® Emerald 300 Lipopolysaccharide Gel Stain Kit (Life Technologies) (bottom panel). LPS with (Smooth) or without (Rough) *O*-antigen moieties are indicated. B. Total LPS content of *Synechocystis* WT EVs was quantified by densitometry analysis (ImageJ). C. Quantification of smooth- to rough-LPS ratio for EVs isolated from *Synechocystis* WT, *Synechocystis* WT cultivated with 4 μM $Cu^{2+}$, and *Synechocystis tolC*-mutant cells. Error bars represent the standard deviations of at least three independent biological replicates. **, $P \leq 0.01$; ***, $P \leq 0.001$, each determined against the WT cultivated under standard growth conditions (0.5 μM $Cu^{2+}$).

(Figs. 6A and B, S3). Furthermore, a significant decrease in the relative amount of smooth- to rough-type LPS could be observed in EVs isolated from cells of both strains exposed to high copper concentrations as compared to EVs isolated from cells cultivated under standard growth conditions (Fig. 6C). This result is similar to the response detected in *Synechocystis* wild-type (Fig. 5C). Altogether, this suggests that the selected Gram-negative bacteria, which include members that occupy different ecological niches respond in a similar manner when exposed to high copper concentrations.

### 3.7. Copper can be detected in isolated cyanobacterial EVs

Finally, to address the possibility of bacterial EVs to work as copper-releasing capsules, the copper amount in vesicles isolated from *Synechocystis* wild-type and *tolC*-mutant strains was analyzed. The choice of strains lies on the fact that the mutant accumulates copper intracellularly already in standard growth conditions (Fig. 1). This means that there is no need to supplement the medium with extra amounts of copper, which could represent a technical challenge when quantifying copper in EVs. Thus, *Synechocystis* wild-type and *tolC*-mutant strains were cultivated in standard growth medium (0.5 μM $Cu^{2+}$), their EVs isolated, thoroughly washed to remove any possible metal binding to the vesicles' surfaces, and later analyzed by atomic absorption spectrometry. Copper could be detected and quantified in EVs samples obtained from both strains. However, the amount of copper quantified in *tolC*-mutant-derived EVs was significantly higher than that of wild-type vesicle fractions, in approximately 3-fold (Fig. 7).

## 4. Discussion

### 4.1. TolC is the outer membrane component of the Synechocystis copper-efflux pump

A *Synechocystis* strain lacking a functional TolC protein has been shown to be severely impaired in secreting several types of molecules, including proteins and antibiotics (Oliveira et al., 2016; Agarwal et al., 2018), drugs (Gonçalves et al., 2018), and even fatty acids (Bellefleur et al., 2019). This phenotype is related to the fact that TolC works as the outer membrane component in multiple tripartite systems (Gonçalves et al., 2019), in which substrate selectivity is defined by the inner membrane component and the periplasmic adaptor protein (Gonçalves et al., 2021; Russo and Zedler, 2021). Thus, TolC can promiscuously

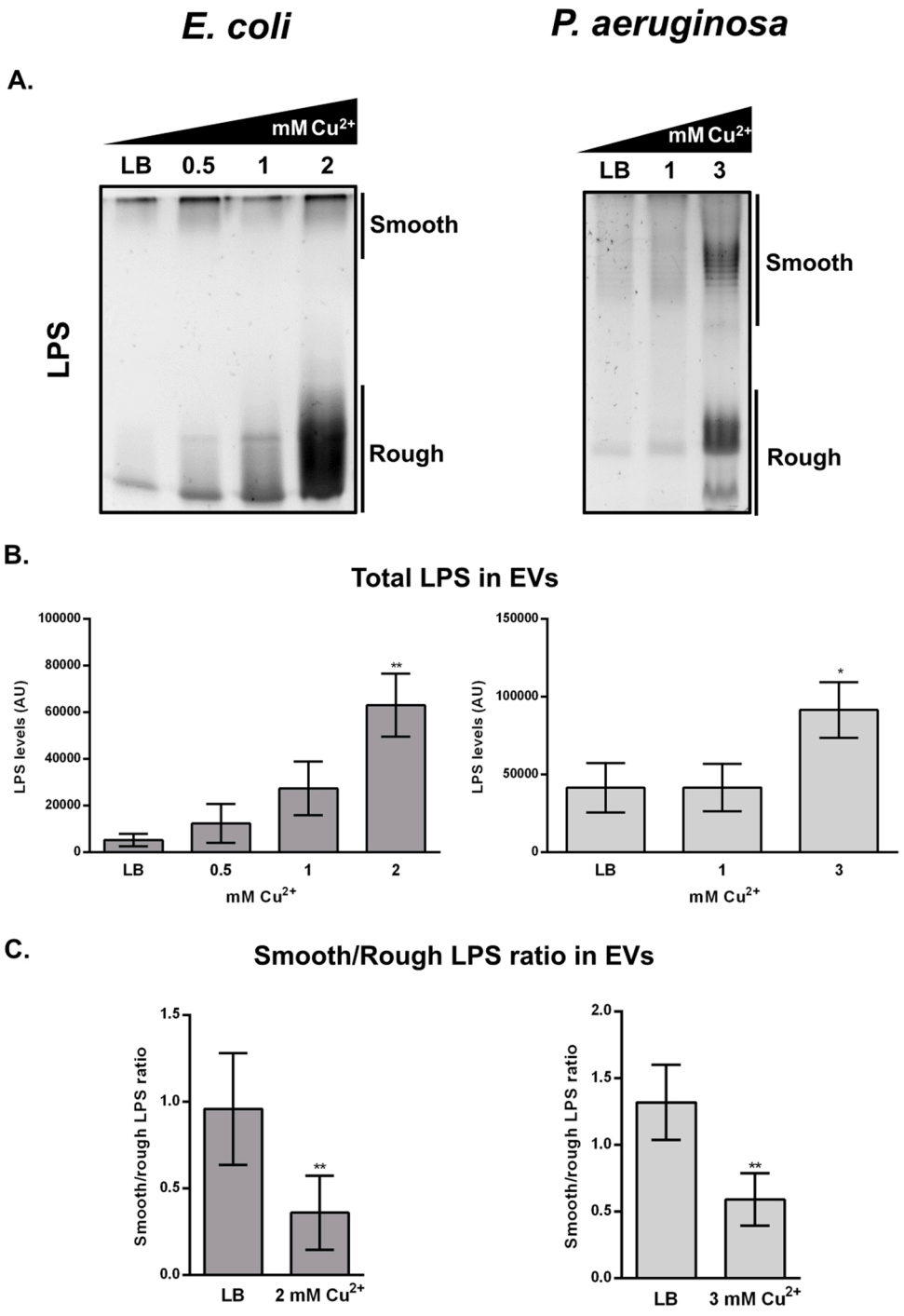


**Fig. 6.** Model bacterial strains produce extracellular vesicles in response to copper supplementation in the medium in a concentration dependent manner. Bacterial strains *Escherichia coli* [strain BL21 (DE3) left-hand panels] and *Pseudomonas aeruginosa* [strain PAO-1 right-hand panels] were cultivated either in LB liquid medium (LB) or in LB liquid medium supplemented with 0.5, 1 and 2 mM $CuSO_4$ for *E. coli*, or 1 and 3 mM $CuSO_4$ for *P. aeruginosa*. After overnight cultivation, EVs were isolated. A. EVs samples were separated by electrophoresis on 16% (w/v) SDS-polyacrylamide gels and lipopolysaccharides (LPS) were stained using the Pro-Q® Emerald 300 Lipopolysaccharide Gel Stain Kit (Life Technologies). LPS with (Smooth) or without (Rough) *O*-antigen moieties are indicated. B. Total LPS content of *E. coli* and *P. aeruginosa* EVs were quantified by densitometry analysis (ImageJ). C. Quantification of smooth- to rough-LPS ratio for EVs isolated from *E. coli* cultivated in LB medium or medium supplemented with 2 mM $Cu^{2+}$, and *P. aeruginosa* cultivated in LB medium or medium supplemented with 3 mM $Cu^{2+}$. Error bars represent the standard deviations of at least three independent biological replicates. *, $P \leq 0.05$; **, $P \leq 0.01$, each determined against the respective strain cultivated in standard LB medium (LB).

assemble with either T1SS-components or RND-efflux pumps to promote the export of molecules directly from the cytoplasm to the extracellular medium. The observation of an intracellular copper accumulation in *Synechocystis tolC*-mutant, accompanied by adaptations related to such copper-imbalance, including upregulation of *copB* transcripts (Fig. 3), high overexpression of CopM (Table 1 and Fig. 3), moderate overexpression of plastocyanin (Table S2), strong and moderate downregulation of cytochrome $c_6$ (PetJ) and of Slr0602, respectively (Table 1), with the latter three proteins part of the PetRP regulon, recently described to be copper-responsive (García-Cañas et al., 2021), highlight the need for the mutant cells to secrete copper.

Taken together, our results support the possibility of TolC working as the outer membrane component of the *Synechocystis* copper-efflux pump. One of the best described copper efflux systems is the *E. coli* CusCFBA transport system (Franke et al., 2003). In this microorganism, CusA is the inner membrane component, CusB the periplasmic adaptor protein, CusC the outer membrane component, and CusF is a soluble periplasmic protein that transports copper in the periplasm to the pump (Nies et al., 2003). Remarkably, despite low sequence similarity, CusC is structurally very similar to TolC (Kulathila et al., 2011), but TolC is not able to physiologically replace CusC in *E. coli*, in respect to conferring resistance to copper ions in vivo (Franke et al., 2003). The most likely reason for this observation would be an inability of TolC to form a functional pump with CusAB (Kulathila et al., 2011). It has been suggested that the linkage among components maintaining copper homeostasis seems evolutionarily driven by protein-protein interactions

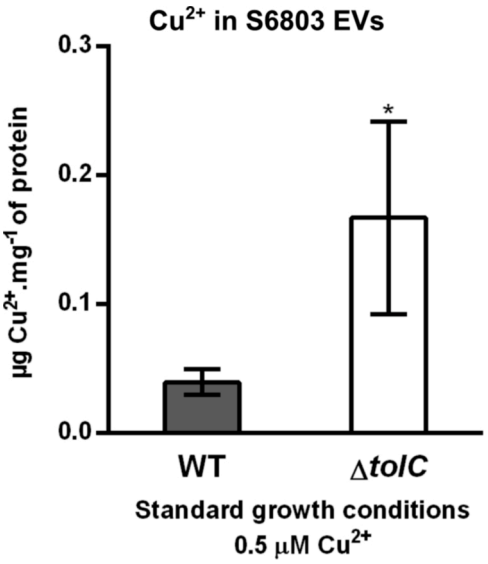


**Fig. 7.** Extracellular vesicles (EVs) isolated from *Synechocystis* sp. PCC 6803 *tolC*-mutant contain more copper than EVs obtained from the wild-type strain, under standard growth conditions. *Synechocystis* sp. PCC 6803 wild-type (WT) and *tolC*-mutant (Δ*tolC*) cells were both cultivated under standard growth conditions (liquid BG11 medium with 0.5 µM $Cu^{2+}$) up to an $OD_{730}$ of 0.8–1.0, and EVs isolated. Prior to analysis, EVs were thoroughly washed in Tris-HCl-EDTA buffer for removal of copper traces derived from the BG11 medium. Amount of copper in isolated EVs was determined by atomic absorption spectrometry, normalized by the total amount of vesicular protein, and expressed in µg $Cu^{2+}$ $mg^{-1}$ of protein. Error bars represent the standard deviations of at least three independent biological replicates. *, $P \leq 0.05$.

rather than by function (Argüello et al., 2013). In fact, a phylogenomic study carried out in γ-proteobacteria showed that copper homeostatic pathways do not behave as evolutionary units, with particular species assembling different combinations of basic functions (Hernández-Montes et al., 2012). This suggests that, depending on the presence or absence of some subunits, bacteria achieve copper homeostasis through the combination of different components and strategies (Hernández-Montes et al., 2012).

In *Synechocystis*, the inner membrane component and the periplasmic adaptor protein of the copper-efflux system have been identified, and are designated as CopA and CopB, respectively (Giner-Lamia et al., 2012). In addition, a gene (*copC*) encoding a small protein of unknown function was found downstream of *copA*, forming the *copBAC* operon. Even though *copC* deletion results in a copper-sensitive phenotype in *Synechocystis*, the role of the encoded protein is not fully understood, but it was proposed to be part of the copper-efflux pump (Giner-Lamia et al., 2012). Nevertheless, the outer membrane component remained unidentified. While CopA and CopB belong to the CusA and to the RND_mfp protein superfamilies, respectively, a search for CusC homologues in selected cyanobacterial genomes retrieves a low number of hits (Ishihara et al., 2020; Nicolaisen et al., 2010), with low sequence similarity. Importantly, the best hits correspond to TolC-like proteins (Nicolaisen et al., 2010), suggesting the absence of CusC in this phylogenetic group. Moreover, these genomic analyses reveal that TolC seems to be the only outer membrane protein in *Synechocystis* capable of interacting with CopAB, and fulfilling the role of exporting copper. Single channel conductance, ion-selectivity studies, and structural modeling have shown that *Synechocystis* TolC protein exhibits different characteristics as compared to the *E. coli* counterpart (Agarwal et al., 2014), which could then be related to its versatile role in mediating the efflux of a wider range of compounds.

### 4.2. EVs as a copper-efflux mechanism in Gram-negative bacteria

In addition to the secretion of various types of (bio)molecules, the *Synechocystis tolC*-mutant has also been shown to significantly release more EVs than the wild-type strain (Oliveira et al., 2016). Similar results have been reported for the pathogenic Gram-negative bacterium *Actinobacillus pleuropneumoniae* (Li et al., 2019). Nevertheless, the biological reasons underlying these observations remained uncharacterized.

When exposed to increasing concentrations of copper, all the Gram-negative bacteria studied in this work, the freshwater cyanobacterium *Synechocystis*, the enteric *E. coli* and the opportunistic pathogen *P. aeruginosa*, responded with production and release of EVs. One possible explanation for this result could be that, during environmental transitions, EVs production facilitates remodeling of cell envelope components, while promoting outer membrane maintenance (Bonnington and Kuehn, 2016). As exposure to high metal concentrations usually results in generation of oxidative stress, EVs production could rid the cell of damaged structural components, including LPS, lipids and proteins. In fact, recent analyses have shown that the *Synechocystis tolC*-mutant studied in this work accumulates high levels of reactive oxygen species compared to the wild-type (Hewelt-Belka et al., 2020), and that despite high activity of superoxide dismutase and catalase (Oliveira et al., 2016), an increase in approximately 50% could be detected in lipid peroxidation in mutant cells compared to the wild-type (Hewelt-Belka et al., 2020). Another reason for the overproduction of EVs in high metal conditions could be to limit the formation of amorphous metal precipitates on the cell surface, as observed in *Leptospira interrogans* when in high iron conditions (Henry et al., 2013). As suggested by the authors, increased EVs production would result in an overall reduction of the surface iron concentration, which in turn would alleviate some of the associated intracellular iron toxicity (Henry et al., 2013).

Although one cannot exclude these possibilities, here we present evidence that supports that EVs work as a copper-efflux system in bacteria, which could partly explain the phenotype observed for the *Synechocystis tolC*-mutant strain. Metal-binding proteins and siderophores have been detected in isolated EVs of various bacterial species, including e.g. *Neisseria meningitidis* (Lappann et al., 2013), *Mycobacterium tuberculosis* (Prados-Rosales et al., 2014), *Enterococcus faecium* (Wagner et al., 2018), and *Staphylococcus aureus* (Askarian et al., 2018). In particular, laccase, a multi-copper oxidase, has been identified in EVs isolated from the fungus *Cryptococcus neoformans* (Rodrigues Marcio et al., 2008). In this work, we detected the copper-binding protein CopM (Giner-Lamia et al., 2015) in EVs isolated from *Synechocystis* (Figs. 3 and 5). CopM is translocated across the inner membrane to the periplasm via the Sec-translocation pathway (Giner-Lamia et al., 2015), and so, its folding occurs in the periplasm. Consequently, CopM binds copper only in the periplasm or in the extracellular medium. Detection of copper in EVs fractions of the *tolC*-mutant strain (and, to a lesser extent, of the wild-type) is consistent with detection of CopM in the respective vesicles. CopM is able to bind both Cu(I) and Cu(II), but it shows higher affinity toward Cu(I), within the femtomolar range (Giner-Lamia et al., 2015), each protein binding 2 Cu(I) ions (Zhao et al., 2016). Considering that the *Synechocystis tolC*-mutant accumulates more copper than the wild-type strain (Fig. 2), it is likely that the copper detected in EVs came from the intracellular metal pool, with EVs production contributing to its secretion, alleviating the cell from excessive copper accumulation.

Determination of smooth-to-rough relative amount of LPS in EVs isolated from wild-type and *tolC*-mutant strain shows a significant increase in rough-type LPS in EVs isolated from the mutant (Fig. 5A and C). Furthermore, quantification of smooth-to-rough LPS in EVs isolated from *Synechocystis* wild-type (Fig. 5C), and *E. coli* and *P. aeruginosa* cells (Fig. 6C) cultivated in the presence of growth-challenging copper concentrations revealed a similar profile, i.e. a decrease in relative amount of smooth-to-rough LPS as compared to cells maintained under standard growth conditions. In addition to the overall increase in EVs production by bacterial cells in response to copper stress, this result highlights that

reshaping LPS composition in released EVs is a common bacterial reaction to such stressful conditions. Jefferies and Khalid (2020) have recently shown that bacterial EVs with a prevalence of smooth-type LPS retain their spherical shape when they interact with membranes of the recipient cell, whereas EVs with shorter LPS (of the rough-type) distort and spread over the membrane surface. Modulations of these interactions led the authors to suggest that spherical-shaped EVs are more likely to be internalized than low-sphericity EVs, which tend to remain on the surface of the cells (Jefferies and Khalid, 2020). In line with Jefferies and Khalid (2020), our results could therefore indicate that EVs released from copper-stressed bacterial cells are less prone to interact with cyanobacterial cells and to deliver their cargo, making the copper present in EVs to be less accessible.

Our working hypothesis to describe copper homeostasis in bacteria, based on the *Synechocystis* model, is therefore presented in Fig. 8. In standard growth conditions, copper homeostasis is reached by the balance between copper uptake and copper efflux. Although the outer membrane components directly involved in copper uptake in cyanobacteria are not fully identified, recent results have shown that highly-abundant porins in the *Synechocystis* outer membrane are responsible for metal uptake (Cardoso et al., 2021; Qiu et al., 2021). Export of copper is supported both by the heavy metal efflux (HME)-pump (CopBAC-TolC complex) and by the secretion of the copper-binding protein CopM. When cells are exposed to medium-high copper concentrations, the key mechanisms for maintaining homeostasis seem to be the copper export systems, with an upregulation of the classical HME-pump and of the metallochaperone CopM. In such stressful conditions, EVs seem also to play a role in copper export. However, in spite of EVs being released by stressed cells in a copper concentration dependent manner, their role in copper export does not seem to be relevant until the cells are exposed to higher copper concentrations. In Figs. 5 and 6, it is possible to see a clear trend in EVs production following gradual increments in copper concentration, but the most significant increase in EVs release is observed when bacterial cells are exposed to the highest copper concentrations tested. This may be interpreted as EVs being one of the last mechanisms activated by bacterial cells to cope with extreme copper concentrations, as copper export via the HME-pump and CopM secretion require less components and are likely less energy demanding than EVs release. CopM-loaded EVs may also work as a copper-uptake system, similar to what has been described for *M. tuberculosis* membrane vesicles in iron acquisition (Prados-Rosales et al., 2014). Thus, CopM-loaded EVs may contribute for copper scavenging from the medium, and so work as a copper sink mechanism. This may be particularly relevant when the bacterium is cultivated in

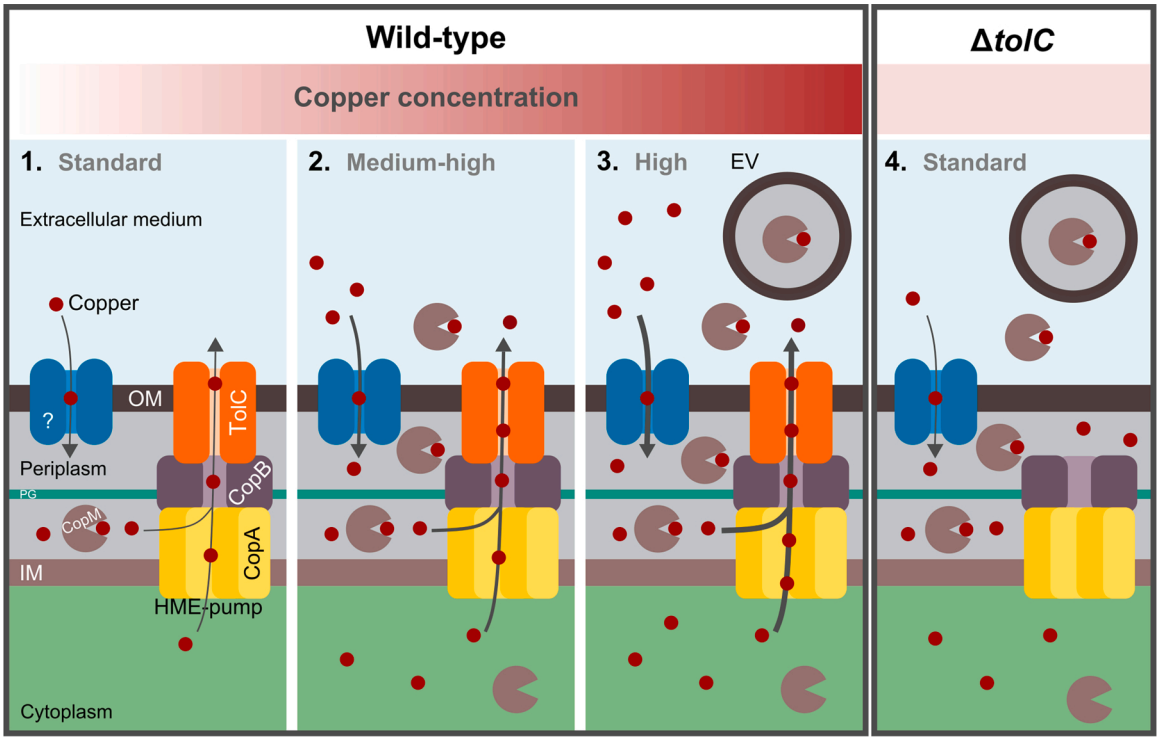


**Fig. 8.** Schematic representation of the copper detoxification mechanisms in Gram-negative bacteria proposed in this work, with a focus on the cyanobacterium *Synechocystis* sp. PCC 6803. In each panel, a diagram showing the bacterial cell envelope, separating the cytoplasm from the extracellular medium, is presented, composed of the two membrane systems [inner membrane (IM), and outer membrane (OM)] limiting the periplasmic space (or periplasm), where the peptidoglycan layer (PG) is found. The outer membrane protein/porin facilitating uptake of copper (red circles) is represented by "?", as its identity in *Synechocystis* remains to be determined. The heavy metal efflux (HME)-pump composed of the inner membrane component CopA, the periplasmic adaptor protein CopB, and the outer membrane protein TolC is also shown. CopC is not represented as it is not clear yet where it is localized. Arrows indicate direction of the metal flux (inward or outward), and their thickness represent flow rate. The metallochaperone CopM is presented in the cytoplasm, where it is synthesized, in the periplasm and in the extracellular medium, where it has been previously detected (Giner-Lamia et al., 2015), and in extracellular vesicles (EV) (this work). 1. In ordinary conditions, copper homeostasis is achieved by a balanced import and export of copper through the outer membrane porin and the HME-pump system, respectively. In addition, CopM complements the copper export system by binding copper in the periplasm and transporting it to the extracellular space, though it does not represent a major outward route, as indicated by the amount of CopM in the medium (Fig. 3). 2. When cells are exposed to medium-high copper concentrations, the metal enters the cell at a higher rate, triggering upregulation of the export mechanisms to ensure metal homeostasis, namely by expression of CopM and of the CopBA subunits of the HME-pump. 3. In high copper concentrations, bacterial copper detoxification mechanisms (HME-pump and CopM) are fully activated to cope with the excessive copper influx. Nevertheless, in conditions in which these systems are not sufficient to deal with copper imbalance, EVs release represents an alternative copper secretion mechanism. 4. In the *Synechocystis tolC*-mutant cultivated under standard conditions, copper homeostasis is compromised, as the HME-pump is functionally inactive due to the lack of the outer membrane protein TolC. Thus, despite the low copper amount in the medium, the cell cannot efficiently balance copper uptake, which leads to activation of the CopM-based secretion system, as well as release of CopM-loaded EVs.

medium supplemented with high copper concentrations: in addition to serving the purpose of exporting copper out of the cell, EVs may also accumulate copper, making it less available for uptake by the cells. Finally, in the *Synechocystis tolC*-mutant, absence of the outer membrane component of the HME-pump severely disrupts copper balance, triggering upregulation of the HME-pump (CopBAC) remaining components and of the CopM system, which seem to be insufficient to deal with an intracellular copper accumulation, even under standard growth conditions. To overcome the stress, CopM-loaded EVs are then released, which help mutant cells to grow similarly to the wild-type (Oliveira et al., 2016).

## 5. Conclusions

In summary, TolC is presented here as the outer membrane component of the HME-pump in *Synechocystis*. As there are several combinations of copper export components in different bacteria, this result opens the possibility of studying TolC as a metal-efflux mediating protein in other relevant bacterial species. Moreover, EVs are suggested to work as a non-classical secretion mechanism to deal with copper-induced stress, which is relevant in the context of using this metal to promote disinfection of, for example, hospital-based surfaces and equipment. However, many questions remain unanswered: can bacterial EVs work as nanocapsules for secretion of other metals than copper? What mechanisms determine EVs packaging with metal-binding proteins under metal stressful conditions, or is it a stochastic mechanism? How does the cell regulate the proportion of smooth-to-rough type LPS in released EVs depending on the condition? Clear answers to these and other questions will surely increase our knowledge on the role played by EVs in bacterial physiology and survival strategies, and help devising technological solutions targeting EVs release to control unwanted bacterial growth.

## Statement of novelty

Copper is an important cofactor in several enzymatic reactions, but when available in high concentrations, it represents a serious risk of causing injury to cells. Here, we present evidence that bacteria use extracellular vesicles (EVs) as copper releasing capsules under copper-induced stressful conditions, representing a breakthrough on the understanding of metal resistance and homeostasis. EVs are discrete, bilayered, nanoscale structures, derived from the bacterial-cell envelope, and released to the extracellular space. The work expands the knowledge on the role played by EVs in bacterial survival strategies, and may help devising technological solutions targeting EVs' release to control unwanted bacterial growth.

## CRediT authorship contribution statement

**Steeve Lima**: Conceptualization, Methodology, Formal analysis, Investigation, Visualization, Writing – original draft. **Jorge Matinha-Cardoso**: Methodology, Formal analysis, Investigation, Visualization, Writing – review & editing. **Joaquín Giner-Lamia**: Methodology, Formal analysis, Investigation, Writing – review & editing. **Narciso Couto**: Methodology, Formal analysis, Investigation, Writing – review & editing. **Catarina C. Pacheco**: Methodology, Formal analysis, Investigation, Visualization, Writing – review & editing. **Francisco J. Florencio**: Supervision, Project administration, Writing – review & editing. **Phillip C. Wright**: Supervision, Funding acquisition, Project administration, Writing – review & editing. **Paula Tamagnini**: Conceptualization, Supervision, Resources, Funding acquisition, Project administration, Writing – review & editing. **Paulo Oliveira**: Conceptualization, Methodology, Formal analysis, Investigation, Visualization, Supervision, Resources, Funding acquisition, Project administration, Writing – original draft, Writing – review & editing.

## Declaration of Competing Interest

The authors declare that they have no known competing financial interests or personal relationships that could have appeared to influence the work reported in this paper.

## Acknowledgments

We wish to express our gratitude to Dr. Cecília Durães and Dr. Ana Rita Pinto for Nanosight EVs analyses. The authors acknowledge the support of the i3S Scientific Platforms "CCGen - Cell Culture and Genotyping", and "Histology and Electron Microscopy" and "Advanced Light Microscopy"; the latter two are members of the national infrastructure Portuguese Platform of Bioimaging (PPBI-POCI-01–0145-FEDER-022122). This work was financed by Fundo Europeu de Desenvolvimento Regional (FEDER) funds through the COMPETE 2020 Operacional Programme for Competitiveness and Internationalisation (POCI), Portugal 2020, and by Portuguese funds through Fundação para a Ciência e a Tecnologia/Ministério da Ciência Tecnologia e Ensino Superior in the framework of the project POCI-01–0145-FEDER-029540 (PTDC/BIA-OUT/29540/2017). Fundação para a Ciência e a Tecnologia is also greatly acknowledged for the PhD fellowship SFRH/BD/130478/2017 (SL), the Assistant Researcher contract CEECIND/00259/2017 (CCP), and FCT Investigator grant IF/00256/2015 (PO). Funding from the EPSRC (EP/E036252/1) and BBSRC (BB/M012166/1) (PCW), and Ministerio de Ciencia, Innovación y Universidades (grant PGC2018-098073-A-I00 MCIU/AEI/FEDER) (JG-L) is also acknowledged.

## Appendix A. Supporting information

Supplementary data associated with this article can be found in the online version at doi:10.1016/j.jhazmat.2022.128594.

## References

Agarwal, R., Whitelegge, J.P., Saini, S., Shrivastav, A.P., 2018. The S-layer biogenesis system of *Synechocystis* 6803: Role of Sll1180 and Sll1181 (*E. coli* HlyB and HlyD analogs) as type-I secretion components for Sll1951 export. *Biochim. Et. Biophys. Acta - Biomembr.* 1860, 1436–1446.

Agarwal, R., Zakharov, S., Hasan, S.S., Ryan, C.M., Whitelegge, J.P., Cramer, W.A., 2014. Structure–function of cyanobacterial outer-membrane protein, Slr1270: Homolog of *Escherichia coli* drug export/colicin import protein, TolC. FEBS Lett. 588, 3793–3801.

Argüello, J., Raimunda, D., Padilla-Benavides, T., 2013. Mechanisms of copper homeostasis in bacteria. Front. Cell. Infect. Microbiol. 3, 73.

Askarian, F., Lapek, J.D., Dongre, M., Tsai, C.-M., Kumaraswamy, M., Kousha, A., et al., 2018. *Staphylococcus aureus* Membrane-Derived Vesicles Promote Bacterial Virulence and Confer Protective Immunity in Murine Infection Models. Front. Microbiol. 9, 262.

Bonnington, K.E., Kuehn, M.J., 2016. Outer Membrane Vesicle Production Facilitates LPS Remodeling and Outer Membrane Maintenance in Salmonella during Environmental Transitions. mBiomBio 7 e01532-16.

EFSA, Arena, M., Auteri, D., Barmaz, S., Bellisai, G., Brancato, A., et al., 2018. Peer review of the pesticide risk assessment of the active substance copper compounds copper(I), copper(II) variants namely copper hydroxide, copper oxychloride, tribasic copper sulfate, copper(I) oxide, Bordeaux mixture. EFSA J. 16, e05152.

Bellefleur, M.P.A., Wanda, S.-Y., Curtiss, R., 2019. Characterizing active transportation mechanisms for free fatty acids and antibiotics in *Synechocystis* sp. PCC 6803. BMC Biotechnol. 19, 5.

Biller, S.J., Schubotz, F., Roggensack, S.E., Thompson, A.W., Summons, R.E., Chisholm, S.W., 2014. Bacterial vesicles in marine ecosystems. Science 343, 183.

Biller, S.J., Lundeen, R.A., Hmelo, L.R., Becker, K.W., Arellano, A.A., Dooley, K., et al., 2021. *Prochlorococcus* extracellular vesicles: molecular composition and adsorption to diverse microbes. Environ. Microbiol.

Biller, S.J., Muñoz-Marín, M.C., Lima, S., Matinha-Cardoso, J., Tamagnini, P., Oliveira, P., 2022. Isolation and characterization of cyanobacterial extracellular vesicles. JoVE 180, e63481.

Bustin, S.A., Benes, V., Garson, J.A., Hellemans, J., Huggett, J., Kubista, M., et al., 2009. The MIQE guidelines: minimum information for publication of quantitative real-time PCR experiments. Clin. Chem. 55, 611–622.

Cardoso, D., Lima, S., Matinha-Cardoso, J., Tamagnini, P., Oliveira, P., 2021. The role of outer membrane protein(s) harboring SLH/OprB-domains in extracellular vesicles' production in *Synechocystis* sp. PCC 6803. Plants 10, 2757.

Djoko, K.Y., Ong, C.-lY., Walker, M.J., McEwan, A.G., 2015. The Role of Copper and Zinc Toxicity in Innate Immune Defense against Bacterial Pathogens. J. Biol. Chem. 290, 18954–18961.

Ferreira, E.A., Pacheco, C.C., Pinto, F., Pereira, J., Lamosa, P., Oliveira, P., et al., 2018. Expanding the toolbox for *Synechocystis* sp. PCC 6803: validation of replicative vectors and characterization of a novel set of promoters. Synth. Biol. 3.

Flombaum, P., Gallegos, J.L., Gordillo, R.A., Rincón, J., Zabala, L.L., Jiao, N., et al., 2013. Present and future global distributions of the marine Cyanobacteria *Prochlorococcus* and *Synechococcus*. Proc. Natl. Acad. Sci. 110, 9824.

Franke, S., Grass, G., Rensing, C., Nies Dietrich, H., 2003. Molecular Analysis of the Copper-Transporting Efflux System CusCFBA of *Escherichia coli*. J. Bacteriol. 185, 3804–3812.

Gaetke, L.M., Chow, C.K., 2003. Copper toxicity, oxidative stress, and antioxidant nutrients. Toxicology 189, 147–163.

García-Cañas, R., Giner-Lamia, J., Florencio, F.J., López-Maury, L., 2021. A protease-mediated mechanism regulates the cytochrome *c*/plastocyanin switch in *Synechocystis* sp. PCC 6803. *Proc. Natl. Acad. Sci.* 118, e2017898118.

Garcia-Pichel, F., Zehr, J.P., Bhattacharya, D., Pakrasi, H.B., 2020. What's in a name? The case of cyanobacteria. J. Phycol. 56, 1–5.

Giner-Lamia, J., López-Maury, L., Florencio, F.J., 2015. CopM is a novel copper-binding protein involved in copper resistance in *Synechocystis* sp. PCC 6803. MicrobiologyOpen 4, 167–185.

Giner-Lamia, J., López-Maury, L., Reyes, J.C., Florencio, F.J., 2012. The CopRS Two-Component System Is Responsible for Resistance to Copper in the Cyanobacterium *Synechocystis* sp. PCC 6803. Plant Physiol. 159, 1806–1818.

Gomes, I.B., Simões, M., Simões, L.C., 2020. Copper surfaces in biofilm control. Nanomaterials 10.

Gonçalves, C.F., Lima, S., Oliveira, P., 2021. Product export in cyanobacteria. Cyanobacteria Biotechnol. 369–406.

Gonçalves, C.F., Lima, S., Tamagnini, P., Oliveira, P., 2019. Chapter 18 - Cyanobacterial Secretion Systems: Understanding Fundamental Mechanisms Toward Technological Applications. In: Mishra, A.K., Tiwari, D.N., Rai, A.N. (Eds.), Cyanobacteria. Academic Press, pp. 359–381.

Gonçalves, C.F., Pacheco, C.C., Tamagnini, P., Oliveira, P., 2018. Identification of inner membrane translocase components of TolC-mediated secretion in the cyanobacterium *Synechocystis* sp. PCC 6803. Environ. Microbiol. 20, 2354–2369.

Henry, R., Lo, M., Khoo, C., Zhang, H., Boysen Reinhard, I., Picardeau, M., et al., 2013. Precipitation of Iron on the Surface of *Leptospira interrogans* Is Associated with Mutation of the Stress Response Metalloprotease HtpX. *Appl. Environ. Microbiol.* 79, 4653–4660.

Hernández-Montes, G., Argüello, J.M., Valderrama, B., 2012. Evolution and diversity of periplasmic proteins involved in copper homeostasis in gamma proteobacteria. BMC Microbiol. 12, 249.

Hewelt-Belka, W., Kot-Wasik, Á., Tamagnini, P., Oliveira, P., 2020. Untargeted Lipidomics Analysis of the Cyanobacterium *Synechocystis* sp. PCC 6803: Lipid Composition Variation in Response to Alternative Cultivation Setups and to Gene Deletion. Int. J. Mol. Sci. 21, 8883.

Ishihara, J.-i., Mekubo, T., Kusaka, C., Kondo, S., Aiba, H., Ishikawa, S., et al. (2020) Critical role of the periplasm in copper homeostasis in Gram-negative bacteria, bioRxiv: 2020.2008.2017.251918.

Jefferies, D., Khalid, S., 2020. To infect or not to infect: molecular determinants of bacterial outer membrane vesicle internalization by host membranes. J. Mol. Biol. 432, 1251–1264.

Kulathila, R., Kulathila, R., Indic, M., van den Berg, B., 2011. Crystal Structure of *Escherichia coli* CusC, the Outer Membrane Component of a Heavy Metal Efflux Pump. PLoS ONE 6, e15610.

Lappann, M., Otto, A., Becher, D., Vogel, U., 2013. Comparative Proteome Analysis of Spontaneous Outer Membrane Vesicles and Purified Outer Membranes of *Neisseria meningitidis*. J. Bacteriol. 195, 4425–4435.

Li, Y., Cao, S., Zhang, L., Yuan, J., Zhao, Q., Wen, Y., et al., 2019. A requirement of TolC1 for effective survival, colonization and pathogenicity of *Actinobacillus pleuropneumoniae*. Microb. Pathog. 134, 103596.

Lima, S., Matinha-Cardoso, J., Tamagnini, P., Oliveira, P., 2020. Extracellular Vesicles: An Overlooked Secretion System in Cyanobacteria. *Life* (*Basel*) 10, 129.

Lopes Pinto, F., Erasmie, S., Blikstad, C., Lindblad, P., Oliveira, P., 2011. FtsZ degradation in the cyanobacterium *Anabaena* sp. strain PCC 7120. J. Plant Physiol. 168, 1934–1942.

McMillan, H.M., Kuehn, M.J., 2021. The extracellular vesicle generation paradox: a bacterial point of view. EMBO J. 40, e108174.

Nicolaisen, K., Hahn, A., Valdebenito, M., Moslavac, S., Samborski, A., Maldener, I., et al., 2010. The interplay between siderophore secretion and coupled iron and copper transport in the heterocyst-forming cyanobacterium *Anabaena* sp. PCC 7120. *Biochim. Et. Biophys. Acta* (*BBA*) - *Biomembr.* 1798, 2131–2140.

Nies, D.H., 2003. Efflux-mediated heavy metal resistance in prokaryotes. FEMS Microbiol. Rev. 27, 313–339.

Oliveira, P., Martins, N.M., Santos, M., Pinto, F., Büttel, Z., Couto, N.A.S., et al., 2016. The versatile TolC-like Slr1270 in the cyanobacterium *Synechocystis* sp. PCC 6803. Environ. Microbiol. 18, 486–502.

Oliveira, P., Pinto, F., Pacheco, C.C., Mota, R., Tamagnini, P., 2015. HesF, an exoprotein required for filament adhesion and aggregation in *Anabaena* sp. PCC 7120. Environ. Microbiol. 17, 1631–1648.

Pardo, Y.A., Florez, C., Baker, K.M., Schertzer, J.W., Mahler, G.J., 2015. Detection of outer membrane vesicles in *Synechocystis* PCC 6803. FEMS Microbiol. Lett. 362.

Pinto, F., Pacheco, C.C., Oliveira, P., Montagud, A., Landels, A., Couto, N., et al., 2015. Improving a *Synechocystis*-based photoautotrophic chassis through systematic genome mapping and validation of neutral sites. DNA Res. 22, 425–437.

Polyviou, D., Machelett, M.M., Hitchcock, A., Baylay, A.J., MacMillan, F., Moore, C.M., et al., 2018. Structural and functional characterization of IdiA/FutA (Tery_3377), an iron-binding protein from the ocean diazotroph *Trichodesmium erythraeum*. J. Biol. Chem. 293, 18099–18109.

Prados-Rosales, R., Weinrick Brian, C., Piqué Daniel, G., Jacobs William, R., Casadevall, A., Rodriguez, G.M., 2014. Role for *Mycobacterium tuberculosis* Membrane Vesicles in Iron Acquisition. J. Bacteriol. 196, 1250–1256.

Qiu, G.-W., Jiang, H.-B., Lis, H., Li, Z.-K., Deng, B., Shang, J.-L., et al., 2021. A unique porin meditates iron-selective transport through cyanobacterial outer membranes. Environ. Microbiol. 23, 376–390.

Rensing, C., McDevitt, S.F., 2013. The Copper Metallome in Prokaryotic Cells. Metallomics and the Cell. Banci, L. (ed). Springer,, Dordrecht.

Rodrigues Marcio, L., Nakayasu Ernesto, S., Oliveira Debora, L., Nimrichter, L., Nosanchuk Joshua, D., Almeida Igor, C., Casadevall, A., 2008. Extracellular Vesicles Produced by *Cryptococcus neoformans* Contain Protein Components Associated with Virulence. Eukaryot. Cell 7, 58–67.

Romanazzi, G., Mancini, V., Foglia, R., Marcolini, D., Kavari, M., Piancatelli, S., 2020. Use of Chitosan and Other Natural Compounds Alone or in Different Strategies with Copper Hydroxide for Control of Grapevine Downy Mildew. Plant Dis.

Russo, D.A., Zedler, J.A.Z., 2021. Genomic insights into cyanobacterial protein translocation systems. Biol. Chem. 402, 39–54.

Schneider, C.A., Rasband, W.S., Eliceiri, K.W., 2012. NIH Image to ImageJ: 25 years of image analysis. Nat. Methods 9, 671–675.

Stanier, R.Y., Kunisawa, R., Mandel, M., Cohen-Bazire, G., 1971. Purification and properties of unicellular blue-green algae (order Chroococcales). Bacteriol. Rev. 35, 171–205.

Toyofuku, M., Nomura, N., Eberl, L., 2019. Types and origins of bacterial membrane vesicles. Nat. Rev. Microbiol. 17, 13–24.

Wagner, T., Joshi, B., Janice, J., Askarian, F., Škalko-Basnet, N., Hagestad, O.C., et al., 2018. *Enterococcus faecium* produces membrane vesicles containing virulence factors and antimicrobial resistance related proteins. J. Proteom. 187, 28–38.

Xu, H., He, E., Peijnenburg, W.J.G.M., Song, L., Zhao, L., Xu, X., et al., 2021. Contribution of pristine and reduced microbial extracellular polymeric substances of different sources to Cu(II) reduction. J. Hazard. Mater. 415, 125616.

Yanong, R.P., 2010. Use of copper in marine aquaculture and aquarium systems. EDIS 2, FA165.

Zhao, S., Wang, X., Niu, G., Dong, W., Wang, J., Fang, Y., et al., 2016. Structural basis for copper/silver binding by the *Synechocystis* metallochaperone CopM. Acta Crystallogr. Sect. D. 72, 997–1005.